

AD-776 672

REGIONAL ATTENUATION OF SHORT-PERIOD
P AND S WAVES IN THE UNITED STATES

Zoltan A. Der, et al

Teledyne Geotech

Prepared for:

Defense Advanced Research Projects Agency

22 January 1974

DISTRIBUTED BY:



National Technical Information Service
U. S. DEPARTMENT OF COMMERCE
5285 Port Royal Road, Springfield Va. 22151

Unclassified

AD446642

SECURITY CLASSIFICATION OF THIS PAGE (When Data Entered)

REPORT DOCUMENTATION PAGE		READ INSTRUCTIONS BEFORE COMPLETING FORM
1 REPORT NUMBER SDAC-TR-74-1	2 GOVT ACCESSION NO.	3 RECIPIENT'S DATA LOG NUMBER
4 TITLE (and Subtitle) REGIONAL ATTENUATION OF SHORT-PERIOD P AND S WAVES IN THE UNITED STATES		5 TYPE OF REPORT & PERIOD COVERED Technical
7 AUTHOR(s) Der, Zoltan A., Nasse, Robert P. and Gurski, John P.		6 PERFORMING ORG. REPORT NUMBER F08606-74-C-0006
9 PERFORMING ORGANIZATION NAME AND ADDRESS Teledyne Geotech 314 Montgomery Street Alexandria, Virginia 22314		10 PROGRAM ELEMENT PROJECT, TASK AREA & WORK UNIT NUMBERS
11 CONTROLLING OFFICE NAME AND ADDRESS Defense Advanced Research Projects Agency Nuclear Monitoring Research Office 1400 Wilson Blvd.-Arlington, Va. 22209		12 REPORT DATE 22 January 1974
14 MONITORING AGENCY NAME & ADDRESS (if different from Controlling Office) VELA Seismological Center 312 Montgomery Street Alexandria, Virginia 22314		13 NUM. OF PAGES 39
16 DISTRIBUTION STATEMENT (of this Report) Approved for Public Release; Distribution Unlimited.		15 SECURITY CLASS. (of this report) Unclassified
17 DISTRIBUTION STATEMENT (of the abstract entered in Block 20, if different from Report)		15a DECLASSIFICATION DOWNGRADING SCHEDULE
18 SUPPLEMENTARY NOTES		
19 KEY WORDS (Continue on reverse side if necessary and identify by block number) Anelastic Attenuation LRSM P Wave S Wave		
Reproduced by NATIONAL TECHNICAL INFORMATION SERVICE U.S. Department of Commerce Springfield VA 22151		
20 ABSTRACT (Continue on reverse side if necessary and identify by block number) Regional distribution of anelastic attenuation beneath the United States was investigated using amplitudes and dominant periods of short period P and S waves originating from deep focus earthquakes in South America and the Circumpacific seismic belt, recorded at LRSM (Long Range Seismic Measurement) stations. The observed regional distribution pattern shows high attenuation in the western United States, including California, and a less		

DD FORM 1 JAN 73 1473 EDITION OF 1 NOV 65 IS OBSOLETE

Unclassified

SECURITY CLASSIFICATION OF THIS PAGE (When Data Entered)

47

Unclassified

SECURITY CLASSIFICATION OF THIS PAGE(When Data Entered)

pronounced high attenuation region in the northeastern United States. This distribution pattern is similar to that reported by Solomon and Toksoz (1970) for long period S waves, but differs from it sufficiently to indicate lateral variations in the frequency dependence of the average crust-upper mantle attenuation across the United States. The relative changes of short period P and S wave amplitudes can be sufficiently explained by assuming a complex shear modulus, no losses in compression are indicated.

Unclassified

SECURITY CLASSIFICATION OF THIS PAGE(When Data Entered)

REGIONAL ATTENUATION OF SHORT-PERIOD P AND S
WAVES IN THE UNITED STATES

Seismic Data Analysis Center Report No.: SDAC-TR-74-1

AFTAC Project No.: VELA VT/4709

Project Title: Seismic Data Analysis Center

ARPA Order No.: 1620

ARPA Program Code No.: 3F10

Name of Contractor: TELEDYNE GEOTECH

Contract No.: F03606-74-C-0006

Date of Contract: 01 July 1973

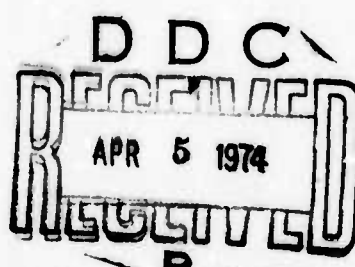
Amount of Contract: \$2,152,172

Contract Expiration Date: 30 June 1974

Project Manager: Royal A. Hartenberger
(703) 836-3882

P. O. Box 334, Alexandria, Virginia 22314

Approved for Public Release; Distribution Unlimited.



ABSTRACT

Regional distribution of anelastic attenuation beneath the United States was investigated using amplitudes and dominant periods of short period P and S waves originating from deep focus earthquakes in South America and the Circumpacific seismic belt, recorded at LRSM (Long Range Seismic Measurement) stations. The observed regional distribution pattern shows high attenuation in the western United States, including California, and a less pronounced high attenuation region in the northeastern United States. This distribution pattern is similar to that reported by Solomon and Toksoz (1970) for long period S waves, but differs from it sufficiently to indicate lateral variations in the frequency dependence of the average crust-upper mantle attenuation across the United States. The relative changes of short period P and S wave amplitudes can be sufficiently explained by assuming a complex shear modulus, no losses in compression are indicated.

TABLE OF CONTENTS

	Page No.
ABSTRACT	
INTRODUCTION	1
DATA	4
S Wave Amplitudes	6
S Wave Periods	15
P Wave Amplitudes	21
P Wave Periods	26
EVALUATION OF THE DATA	27
DISCUSSION	30
ACKNOWLEDGEMENTS	35
REFERENCES	36

LIST OF FIGURES

Figure No.	Figure Title	Page No.
1	Geographical distribution of S wave amplitudes corrected for distance dependence for the Peru-Brazil border event.	11
2	Geographical distribution of S wave amplitudes corrected for distance dependence for the NW Kuriles event.	13
3	Geographical distribution of S wave amplitudes corrected for distance dependence for the Sea of Okhotsk event.	14
4	Geographical distribution of S wave amplitudes corrected for distance dependence for the Western Brazil event.	16
5	Dominant S wave period plotted against S wave amplitude for the Peru-Brazil border event. Dashed line is the assumed boundary between stations with high and low attenuation.	17
6	Dominant S wave period plotted against S wave amplitude for the NW Kurile event. Dashed line is the assumed boundary between stations with high and low attenuation.	18
7	Dominant S wave period plotted against S wave amplitude for the Sea of Okhotsk event. Dashed line is the assumed boundary between stations with high and low attenuation.	19

LIST OF FIGURES (Continued)

Figure No.	Figure Title	Page No.
8	Dominant S wave period plotted against S wave amplitude for the Western Brazil event. Dashed line is the assumed boundary between stations with high and low attenuation.	20
9	P amplitudes plotted against S amplitudes for the Peru-Brazil border event. Dashed line is the boundary between stations with high and low attenuation.	22
10	P amplitudes plotted against S amplitudes for the NW Kuriles event. Dashed line is the boundary between stations with high and low attenuation.	23
11	P amplitudes plotted against S amplitudes for the Sea of Okhotsk event. Dashed line is the boundary between stations with high and low attenuation. Solid line is the approximate relationships between P and S amplitudes assuming losses in shear only.	24
12	P amplitudes plotted against S amplitudes for the Western Brazil event. Dashed line is the boundary between stations with high and low attenuation. Solid line is the approximate relationships between P and S amplitudes assuming losses in shear only.	25
13	Distribution of attenuation under the United States based on all events.	32

LIST OF TABLES

Table No.	Table Title	Page No.
1	Events Studied	5
2/a	Peru-Brazil Border Event	7
2/b	NW Kuriles Event	8
2/c	Sea of Okhotsk Event	9
2/d	Western Brazil Event	10
3	Classification of LRSM Sites with Report to Attenuation Characteristics	29

INTRODUCTION

As a result of geophysical investigations over the past decade, the existence of lateral variations in the crust and upper mantle has been well established. However, many questions concerning the exact lateral variation of the physical properties of the Earth remain to be answered. Particularly sensitive to such lateral variations are the spectral amplitudes of short-period body waves from teleseismic events.

In this study the variation of short-period P and S wave amplitudes across the United States is investigated. While the amplitudes of short-period waves can be expected to be affected by local structure at the recording sites and by scattering and multipathing due to inhomogeneities, for the most part the general pattern of the amplitudes as observed across the United States is believed to correspond to attenuation in the upper mantle and lower crust after a correction is made for distance effects. Dominant periods of the waves will also be considered as an additional diagnostic. Comparisons of the observed amplitude pattern with the results of other geophysical studies support this belief. The term attenuation is therefore used in this paper in discussing the relative amplitude decrease and changes in dominant wave period although, for some recording sites, it should be understood that other effects may be important.

The measurement of seismic wave attenuation has structural implications since the upper mantle low-velocity channel is generally associated with the region of high attenuation (low Q). Therefore the extent and thickness of the low-velocity channel may possibly be indicated by the geographical variation in the attenuation of the short-period body waves. If this is so, then such information could be used to determine if the large low-velocity channel beneath the Western United States thins gradually towards the east as suggested by Green and Hales (1968) or if it abruptly decreases in size as proposed by Masse' (1973).

Variation of the attenuation with frequency is diagnostic of the attenuation mechanism and, in this respect, data from this study provides new information for the short-period end of the spectrum. The dependence of attenuation on frequency is obvious for, as noted by Solomon et al (1970), short-period P and S waves would not be observed at all if the Q values appropriate for long-period S and surface waves were independent of frequency. Therefore, the Q of seismic waves can be expected to increase slowly with increasing frequency from the values determined using long-period observations. This increase of Q with frequency has also been found in the study of long-period S waves by Sato and Espinosa (1967).

Attenuation of seismic waves in the upper mantle is usually attributed to the presence of melt in the rocks (Jackson, 1969; and Walsh, 1968). The frequency

dependence of attenuation is indicative of the percentage and viscosity of the melt, the shape of inclusions, and the values of various parameters of geophysical interest. Since all of these parameters can change from area to area, the frequency dependence of attenuation can also change. Therefore attenuation maps for various period ranges can give a considerable amount of information about the upper mantle.

Attenuation information for long-period P and S waves and long-period surface waves is available from a number of previous studies (Solomon and Toksöz, 1970; Solomon, 1972; Anderson and Archambeau, 1964; and Anderson et.al., 1965). Variations of short-period attenuation have been used to study structure in subduction zones (Oliver and Isacks, 1967), but studies of short-period P and S wave attenuation over wide areas are few. Studies such as those by Molnar and Oliver (1970) and Sutton et al (1967) involve guided waves which tend to give at best an average attenuation value over the path for only the crust and uppermost mantle immediately below the Mohorovičić discontinuity, possibly modified by variations in the waveguide.

DATA

Four deep earthquakes have been selected for analysis in this study. Epicentral data for these events are given in Table I. Two of these earthquakes occurred in South America and two on the far side of the circum-pacific belt of earthquakes in the Kurile Islands region. This distribution of epicenters assures that azimuthal effects due to source or near-source structure radiation patterns can be minimized, as it is unlikely that sources in the two regions would behave the same way. Deep earthquakes with focus below most of the asthenosphere were chosen since presumably energy from these events can freely radiate into the high Q portion of the mantle and thus most attenuation will occur in the ascending part of the ray path. Short-period recordings at all available stations which were part of the Long Range Seismic Measurements Program (LRSM) within the continental United States have been analyzed. Maximum peak-to-peak amplitudes of short-period P and S waves and the dominant periods of the waves at the points of amplitude measurements were read on all available seismometer components. Where no wave could be seen, the noise background was read to establish an upper amplitude limit for the wave. The amplitudes read were corrected for the instrument magnification at the dominant period of the waves. The dominant period of S waves was defined as the mean of the readings on the three components. An approximate distance correction for both P and S waves was also applied.

TABLE 1
EVENTS STUDIED

REGION	LATITUDE	LONGITUDE	MAGNITUDE	DEPTH KM	ORIGIN TIME
Peru-Brazil Border	9.1S	71.4W	4.9	585	19:54:09.4
N. W. Kuriles	52.5N	153.6E	5.6	400	04:37:26.9
Sea of Okhotsk	46.6N	144.6E	5.5	383	20:08:28.5
Western Brazil	7.7S	71.2E	5.4	626	16:41:33.4

based on the formula $A \sim \exp(-0.0148 \Delta^\circ)$. This correction was derived from the smoothed Gutenberg body wave magnitude B factors, and was used to reduce the amplitudes to the equivalent amplitude at the arbitrarily chosen distance of 50° . The amount of the distance correction is minor compared to the amplitude variations observed, and never exceeds a factor of 1.5. The S wave amplitudes were then determined by taking the square root of the sum of the squared component amplitude readings. The raw amplitudes as well as amplitudes with distance corrections are given in Table 2. All the figures show the amplitudes corrected for distance effects for each event.

S Wave Amplitudes

Figure 1 shows the amplitudes for the Peru-Brazil border event. At the time of this event a profile of LRSM stations existed which stretched from Texas to California. Especially striking in Figure 1 is the abrupt decrease of S wave amplitudes between AZTX and RTNM. This seems to mark the boundary between the high Q eastern region and the low Q western region. The boundary was placed in roughly the same area by Solomon and Toksöz (1970), but they used data from only two WWSSN stations, ALQ and JCT, in this region and could not define the boundary as precisely. This reduction in S wave amplitude coincides with the region of recent volcanism in northeastern New Mexico. A notable difference between the amplitude pattern shown in Figure 1

TABLE 2/a
Peru-Brazil Border Event

Station	P Amplitude $m\mu$	Reduced P Amplitude $m\mu$	P Period Sec.	S Amplitude $m\mu$	Reduced S Amplitude $m\mu$	S Period Sec.
APOK	27.4	27.6	0.80	3.2	3.2	0.90
AZTX	20.5	21.4	0.60	6.3	6.6	0.40
BXUT	14.7	16.7	0.80	2.9	3.2	1.70
CPCL	2.9	3.3	0.60	< 2.6	< 3.0	-
CUNV	7.8	9.4	1.00	-	-	-
DRCO	4.5	5.1	0.70	< 0.5	< 0.6	-
DUOK	-	-	1.00	5.1	5.6	1.00
EBMT	-	-	1.00	3.1	3.7	1.03
EUAL	25.9	23.9	0.80	7.2	7.0	0.70
FRMA	17.7	21.6	0.60	6.1	7.5	1.40
GIMA	45.8	55.7	0.60	<19.6	<23.8	-
GVTX	34.0	33.2	0.50	<10.3	<10.0	-
HETX	26.4	24.8	0.60	< 7.2	< 6.8	-
HHND	37.6	45.3	0.60	<17.0	<20.6	-
HLID	5.4	6.7	0.80	-	-	-
KNUT	-	-	1.00	< 5.2	< 6.1	-
LCNM	2.2	2.3	0.60	< 2.6	< 2.8	-
LVLA	<46.3	<42.0	0.30	<67.7	<61.4	-
MNNV	7.4	9.2	1.50	< 1.4	< 1.8	-
MVCL	0.2	0.2	0.70	2.3	3.0	-
PYND	19.3	23.4	0.60	5.2	3.9	0.60
RTNM	6.0	6.5	0.60	< 1.6	< 1.9	-
SKTX	32.0	32.9	0.70	< 3.0	< 8.3	1.15
TDNM	2.8	2.1	0.60	0.3	0.5	-
WINV	12.2	15.4	0.60	2.4	3.0	2.20

TABLE 2/b
NW. Kuriles Event

Station	P Amplitude $\mu\mu$	P Amplitude $\mu\mu$	Reduced P Period Sec.	S Amplitude $\mu\mu$	S Amplitude $\mu\mu$	Reduced S Period Sec.
BLWV	30.1	46.0	0.60	370.4	565.6	3.86
BXUT	-	-	1.00	94.8	118.7	3.13
DHNY	99.3	148.1	0.70	70.5	105.1	1.95
DPCO	13.0	16.5	0.70	132.2	168.0	3.36
EBMT	-	-	1.00	165.2	199.4	3.56
EKNV	-	-	1.00	31.2	36.6	2.23
EUAL	53.6	83.6	0.80	224.0	349.5	2.50
FAMA	-	-	1.00	507.1	591.4	3.60
GIMA	50.0	58.5	0.70	442.6	518.3	2.20
GVTX	39.2	57.0	0.70	73.3	106.6	2.65
HNME	77.0	112.5	0.60	94.6	138.2	2.50
HHND	105.4	125.6	0.80	196.4	234.2	1.46
JELA	17.8	27.4	0.80	174.5	267.6	2.95
KMCL	16.9	20.4	0.60	41.9	49.6	2.76
KNUT	-	-	1.00	69.5	85.2	3.16
LCNM	13.4	18.3	0.50	55.7	75.7	3.03
LSNH	32.5	47.8	0.60	272.0	400.8	2.33
MNNV	-	-	1.00	51.2	59.2	2.36
P1WY	17.7	21.0	0.90	140.1	166.2	2.53
RKON	-	-	1.00	74.3	89.5	2.00
RYND	-	-	1.00	621.8	784.8	2.33
TKWA	-	-	1.00	36.7	37.9	2.40
TRNM	27.9	36.2	0.70	102.2	132.9	3.50

TABLE 2/c
Sea of Okhotsk Event

Station	P Amplitude $\mu\mu$	Reduced P Amplitude $\mu\mu$	P Period Sec.	S Amplitude $\mu\mu$	Reduced S Amplitude $\mu\mu$	S Period Sec.
BLWV	15.8	27.4	0.70	22.0	38.1	2.40
BRPA	21.8	37.4	0.60	18.0	30.9	2.36
DHNY	35.5	60.2	0.60	11.7	19.9	2.35
DRCO	11.4	16.4	0.80	17.2	24.7	2.96
EBMT	32.7	44.7	0.70	16.7	22.9	1.96
EUAL	54.1	95.7	0.70	26.9	47.7	0.80
FKNV	16.3	21.6	0.90	< 1.8	< 2.4	-
FOTX	-	-	1.00	20.3	32.8	2.80
FRMA	23.7	31.3	1.00	< 10.1	< 13.4	-
GIMA	52.2	69.3	1.20	< 6.4	< 8.4	-
GVTX	21.7	36.0	0.80	< 31.2	< 51.7	-
HHND	42.0	57.6	0.60	< 10.0	< 13.7	-
HLID	-	-	1.00	1.8	2.2	1.45
HNME	32.1	53.1	0.70	10.4	17.3	2.30
JELA	< 18.4	< 32.1	0.40	< 22.9	< 40.0	-
KNUT	17.3	24.0	1.00	< 3.9	< 1.2	-
LCNM	7.5	11.2	0.80	5.1	7.9	2.53
LGAZ	37.3	53.5	0.80	11.0	15.9	2.40
LSNH	10.1	16.9	0.60	5.3	8.9	2.00
MNNV	11.2	14.5	0.70	< 1.5	< 1.9	-
RKON	29.9	40.9	0.60	9.6	13.0	1.36
RTNM	16.3	24.2	0.80	13.0	19.3	3.00
RYND	99.7	133.6	0.60	71.4	95.7	2.00
SNAZ	15.2	21.9	0.80	22.9	33.1	3.00
WOAZ	25.4	36.6	0.80	12.3	17.7	2.40
WSND	33.2	44.5	0.90	41.3	55.3	2.00

TABLE 2/J
Western Brazil Event

Station	P Amplitude m_{μ}	Reduced P Amplitude m_{μ}	P Period Sec.	S Amplitude m_{μ}	Reduced S Amplitude m_{μ}	S Period Sec.
BLWV	107.6	101.9	0.50	50.1	47.5	1.50
BRPA	-	-	1.00	12.1	11.7	1.40
DHNY	22.9	22.8	0.50	< 33.5	< 33.4	-
DRCO	17.2	19.0	0.60	3.0	3.3	1.43
FOTX	-	-	1.00	30.5	30.0	1.30
GEAZ	7.0	7.7	0.60	22.7	24.8	2.66
GPMN	176.6	193.1	0.50	117.0	127.9	1.86
GVTX	77.7	74.7	0.60	76.2	73.3	1.63
HDPA	42.5	41.2	0.40	< 20.3	< 19.7	-
HLID	12.3	15.2	0.50	< 14.2	< 17.7	-
HNME	13.8	14.2	0.80	< 16.8	< 17.3	-
KNUT	-	-	1.00	55.5	63.6	2.50
LCNM	8.7	9.0	0.50	11.5	11.9	1.36
LGAZ	23.3	25.8	0.60	23.3	25.7	3.13
LSNH	26.5	27.3	0.60	< 20.1	< 20.7	-
MNNV	7.5	9.1	0.80	2.1	2.5	2.00
NLAZ	19.5	21.5	0.60	20.8	23.0	2.65
RKON	54.9	65.1	0.50	25.8	30.6	1.13
RTNM	13.5	14.3	0.60	43.7	46.5	2.86
RYND	-	-	1.00	109.7	130.5	1.65
SGAZ	12.9	14.4	0.60	11.1	12.4	2.40
VOTD	-	-	1.00	32.1	32.1	1.20

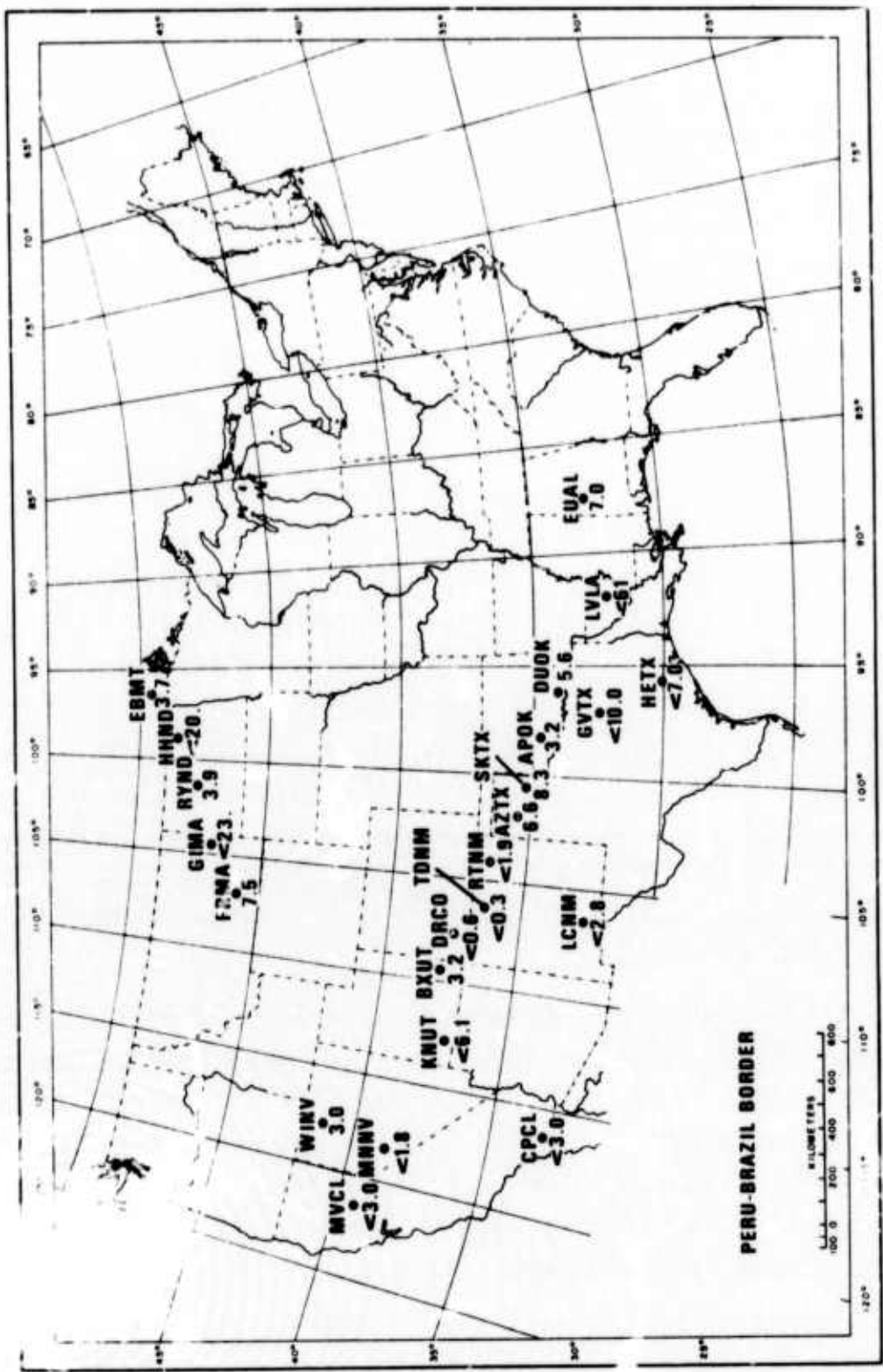


Figure 1. Geographical distribution of S wave amplitudes corrected for distance dependence for the Peru-Brazil border event.

and the attenuation picture given by Solomon and Toksöz (1970) may be seen for California. In Figure 1 all the short-period S amplitudes remain low in California which is not the case for the long-period amplitudes observed by Solomon and Toksöz. All S amplitudes in the Basin and Range Province and in the Colorado Plateau region are low.

Figure 2 shows the amplitudes derived from the Kurile Island event. This figure shows the same general picture in the western half of the United States as the first figure, with low S amplitudes predominating. Apparently unusual values were found for GVTX and RKON. HNME and DHNY also have low amplitudes, which lends some support to the proposed low Q region in the north-eastern United States made by Solomon and Toksöz. However LSNH has a high amplitude value which does not agree with this suggestion. The boundary separating the high and low Q regions seems to be situated between stations PIWY and FRMA in the northwestern United States. The LRSM station KMCL has a low S amplitude which is in disagreement with the high Q western region assumed by Solomon and Toksöz.

Figure 3 shows the S wave results for the Sea of Okhotsk event. This map shows very low amplitude values for MNNV, EKNV, KNUT, and HLID. For the rest of the stations the contrast between eastern and western stations is as great, although the tendency of western stations to be smaller is clear. The boundary indicated by this event in the northwest should fall between GIMA

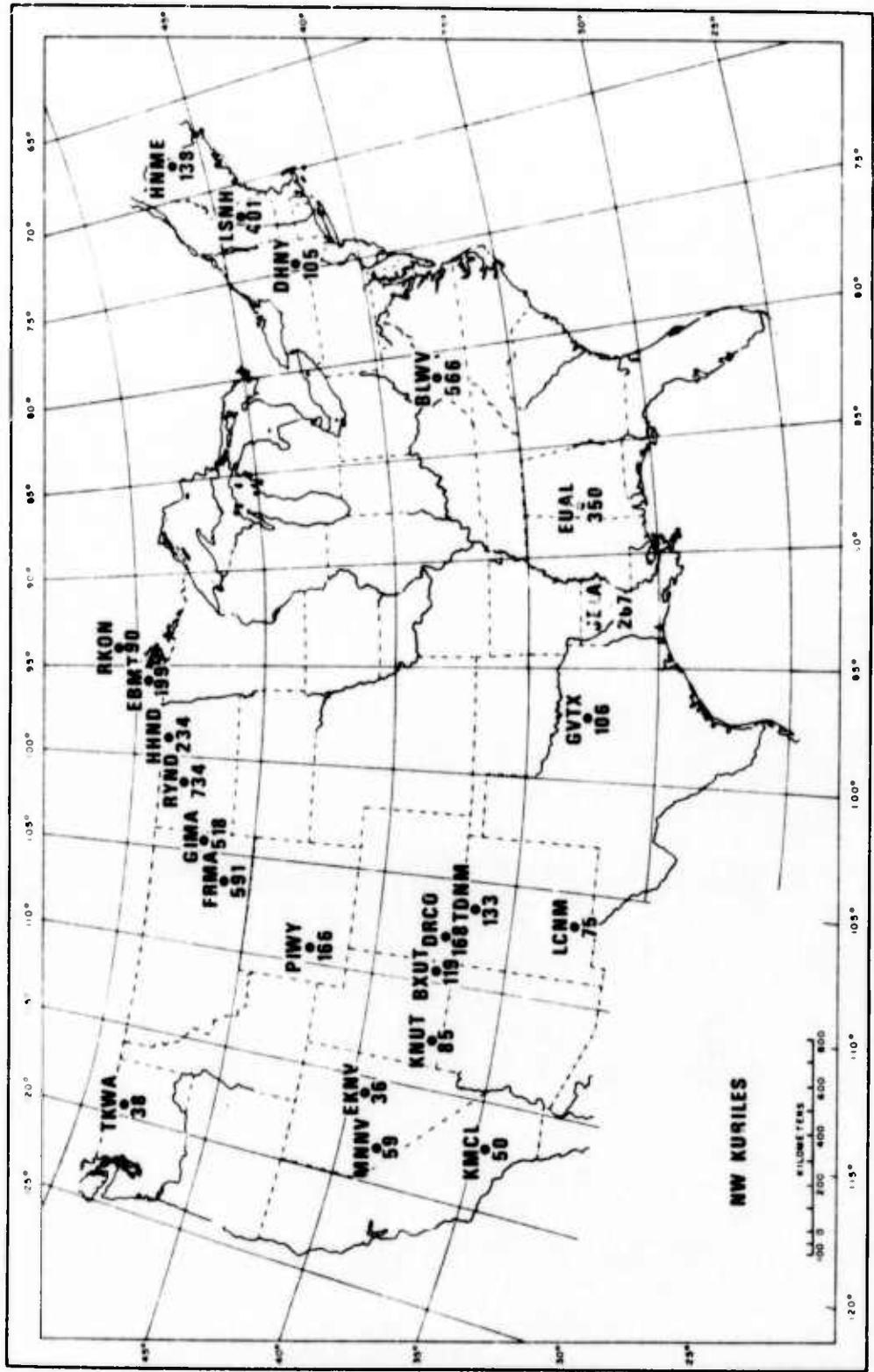


Figure 2. Geographical distribution of S wave amplitudes corrected for distance dependence for the NW Kuriles event.

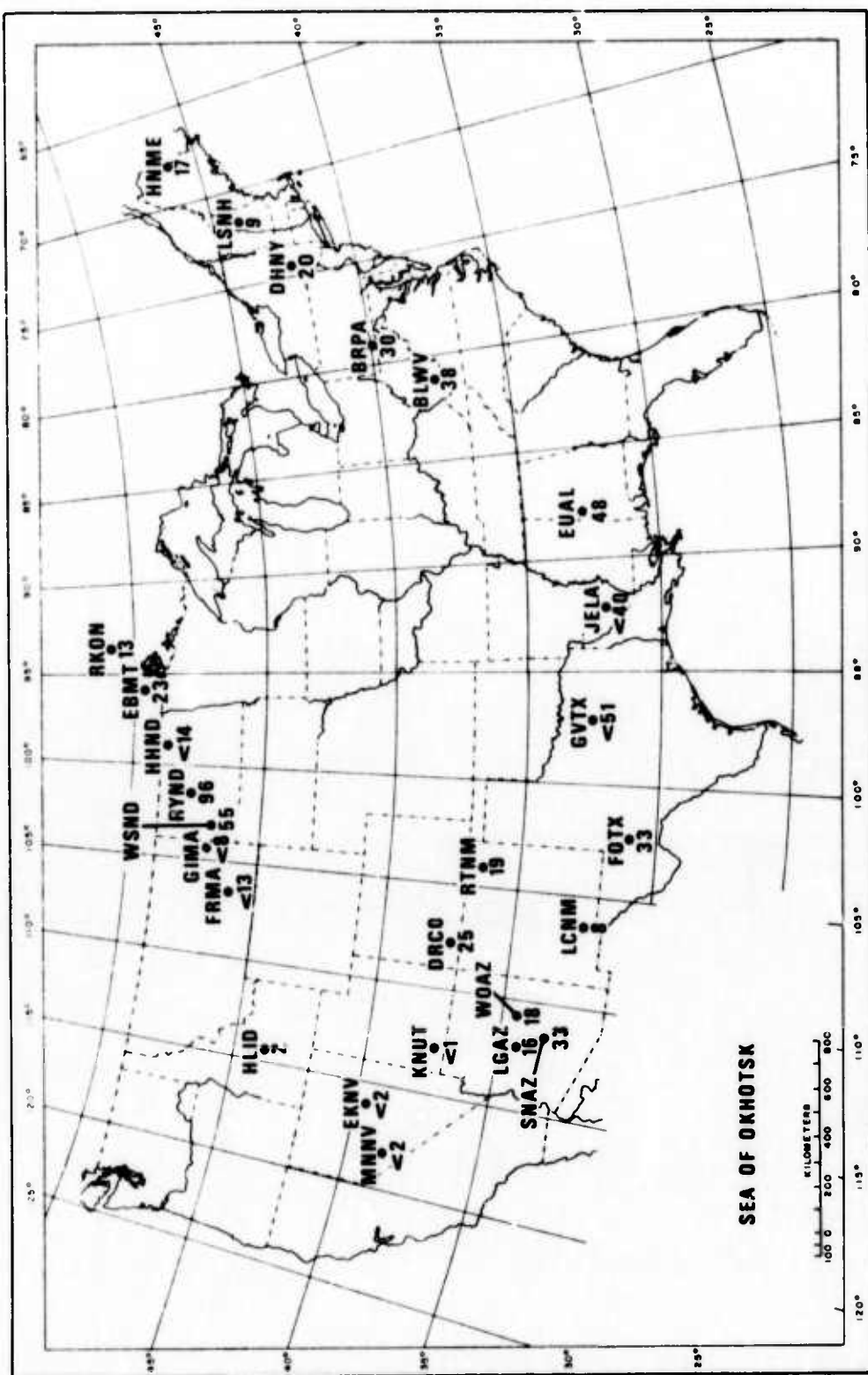


Figure 3. Geographical distribution of S wave amplitudes corrected for distance dependence for the Sea of Okhotsk event.

and TSND in contrast to the previous event. The amplitude value at RKON is low again. The northeastern stations tend to have low S wave amplitudes.

The S wave amplitudes for the Western Brazil event (Figure 4) indicate roughly the same behavior as the other events, with about the same amount of scatter. As for the previous events, there are a few stations which are inconsistent with the general patterns such as RKON, BRPA, and VOIO which have low values and KNUT which has a high value.

S Wave Periods

The periods of the observed S waves as given in Table 2 are averages of the observed periods from all components. The average error of period readings is quite large and can amount to 0.5 second. Figures 5 through 8 show the average S periods plotted against the logarithms of S amplitudes for the four events. The philosophy behind these plots is that since both the periods and amplitudes are diagnostic of regional attenuation the combination of both can be used to eliminate inconsistencies due to reading errors and due to some of the effects of local near-surface resonances and multipathing which can cause considerable variation in short-period body wave amplitudes (Mack, 1970). In general, low amplitudes should correlate with long periods and vice versa. The plots agree with these expectations.

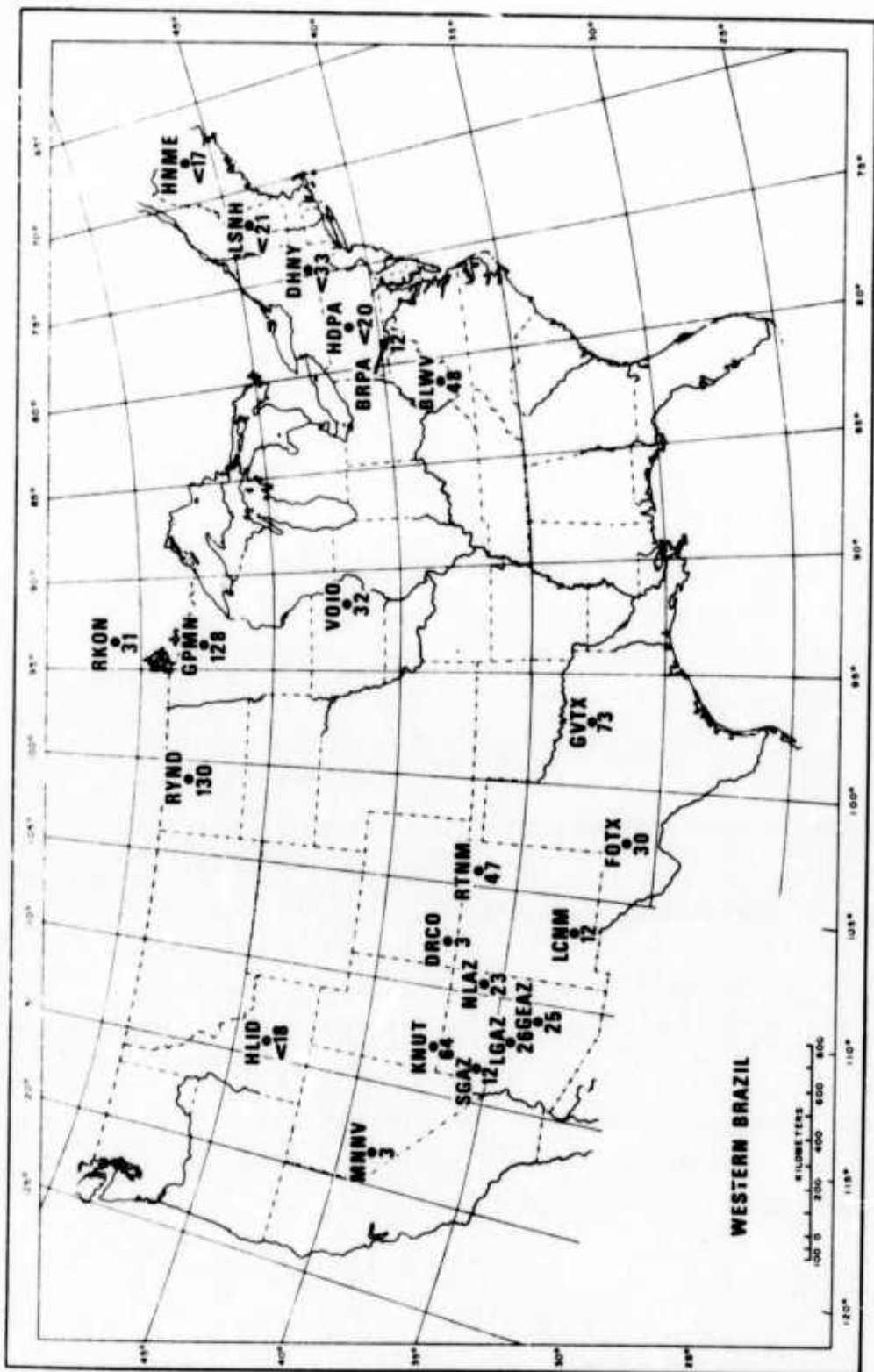


Figure 4. Geographical distribution of S wave amplitudes corrected for distance dependence for the Western Brazil event.

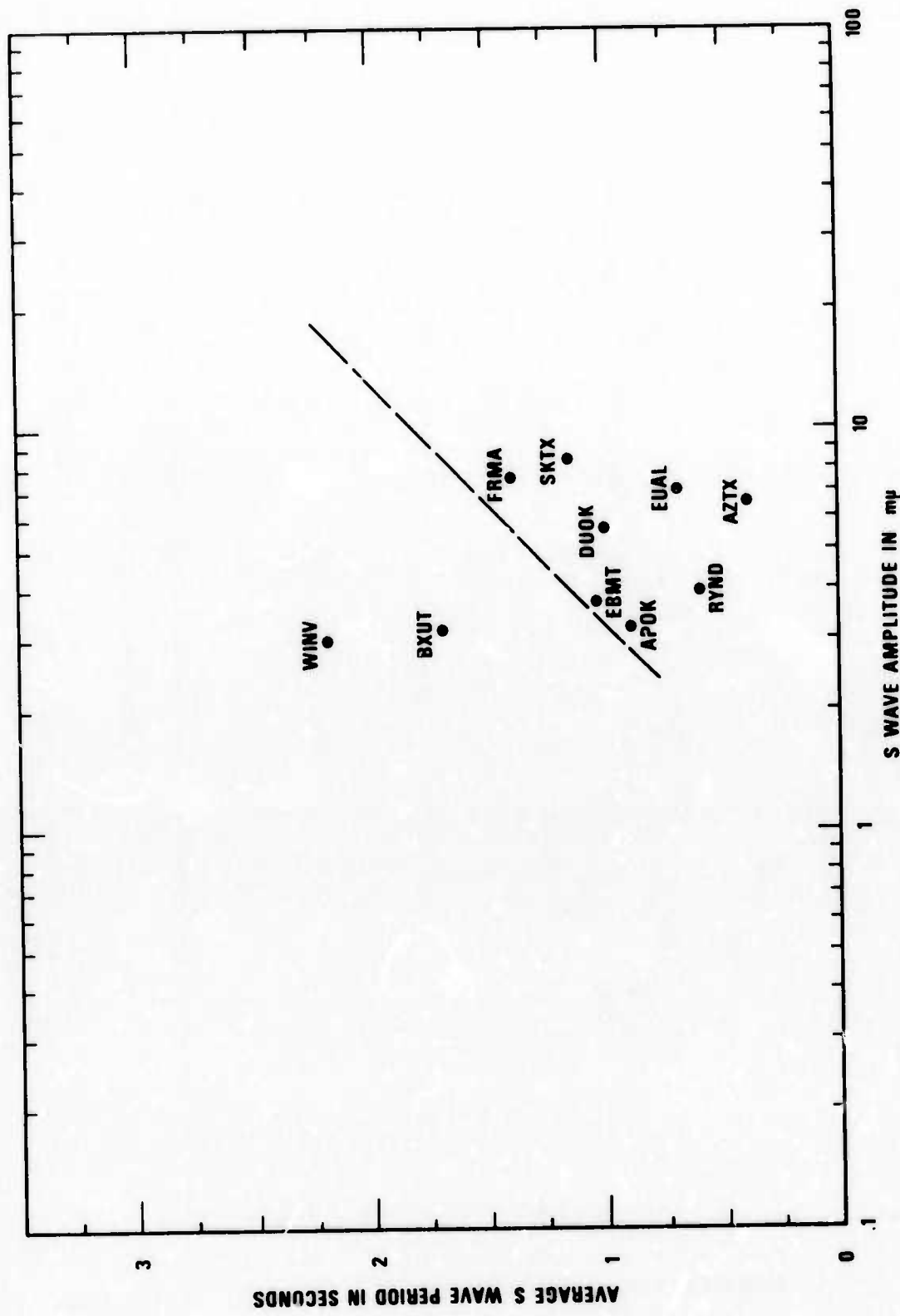


Figure 5. Dominant S wave period plotted against S wave amplitude for the Peru-Brazil border event. Dashed line is the assumed boundary between stations with high and low attenuation.

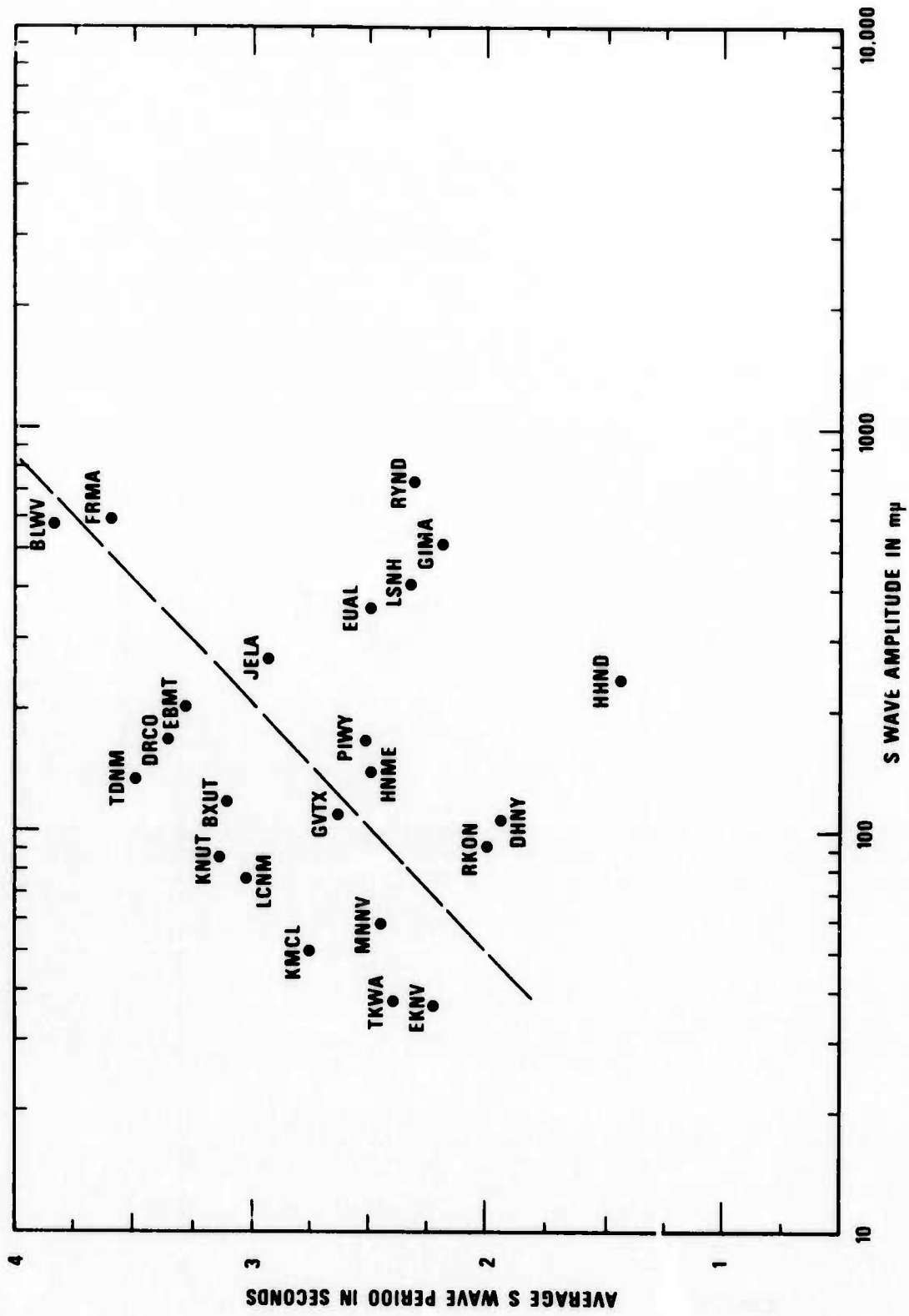


Figure 6. Dominant S wave period plotted against S wave amplitude for the NW Kurile event. Dashed line is the assumed boundary between stations with high and low attenuation.

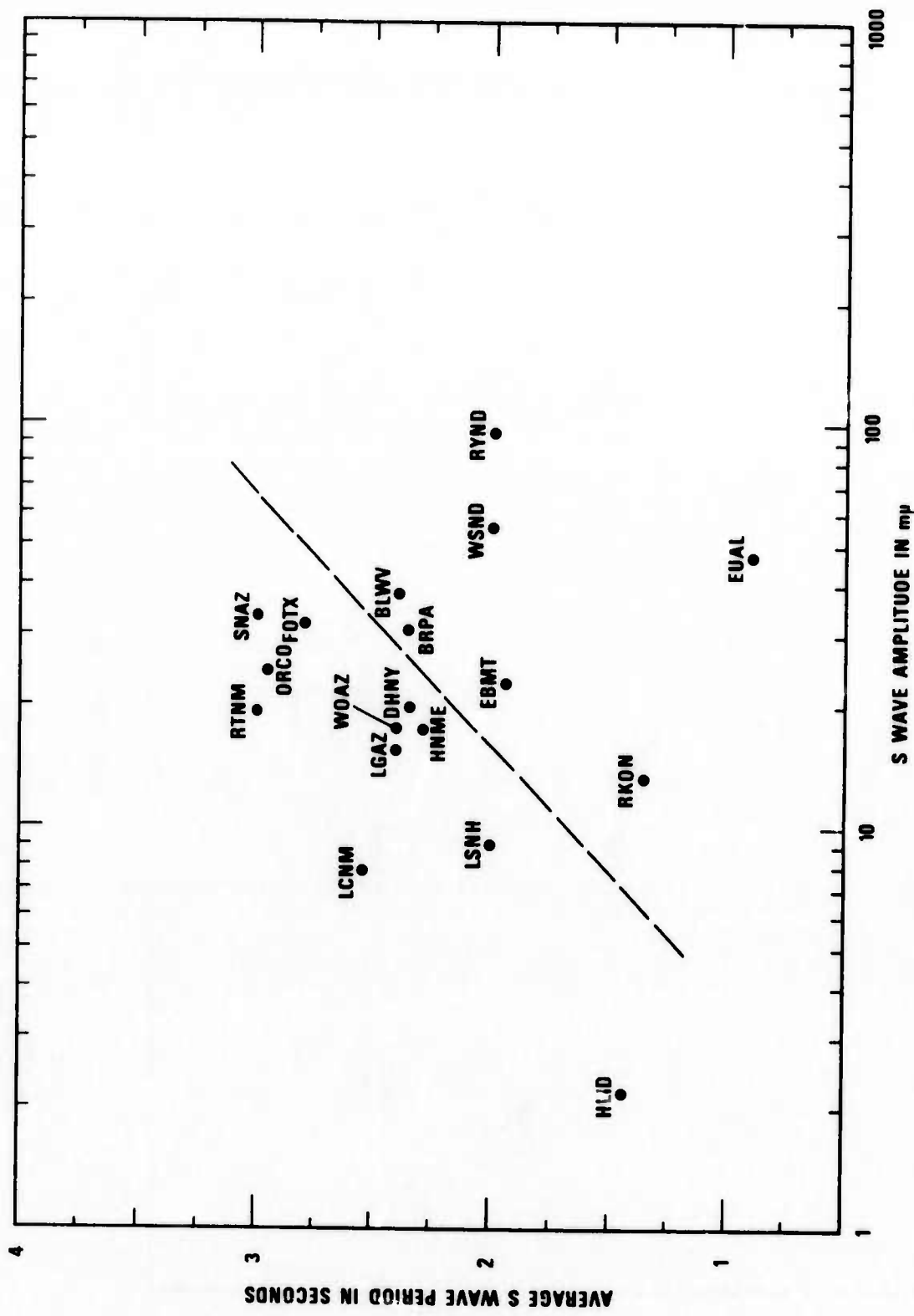


Figure 7. Dominant S wave period plotted against S wave amplitude for the Sea of Okhotsk event. Dashed line is the assumed boundary between stations with high and low attenuation.

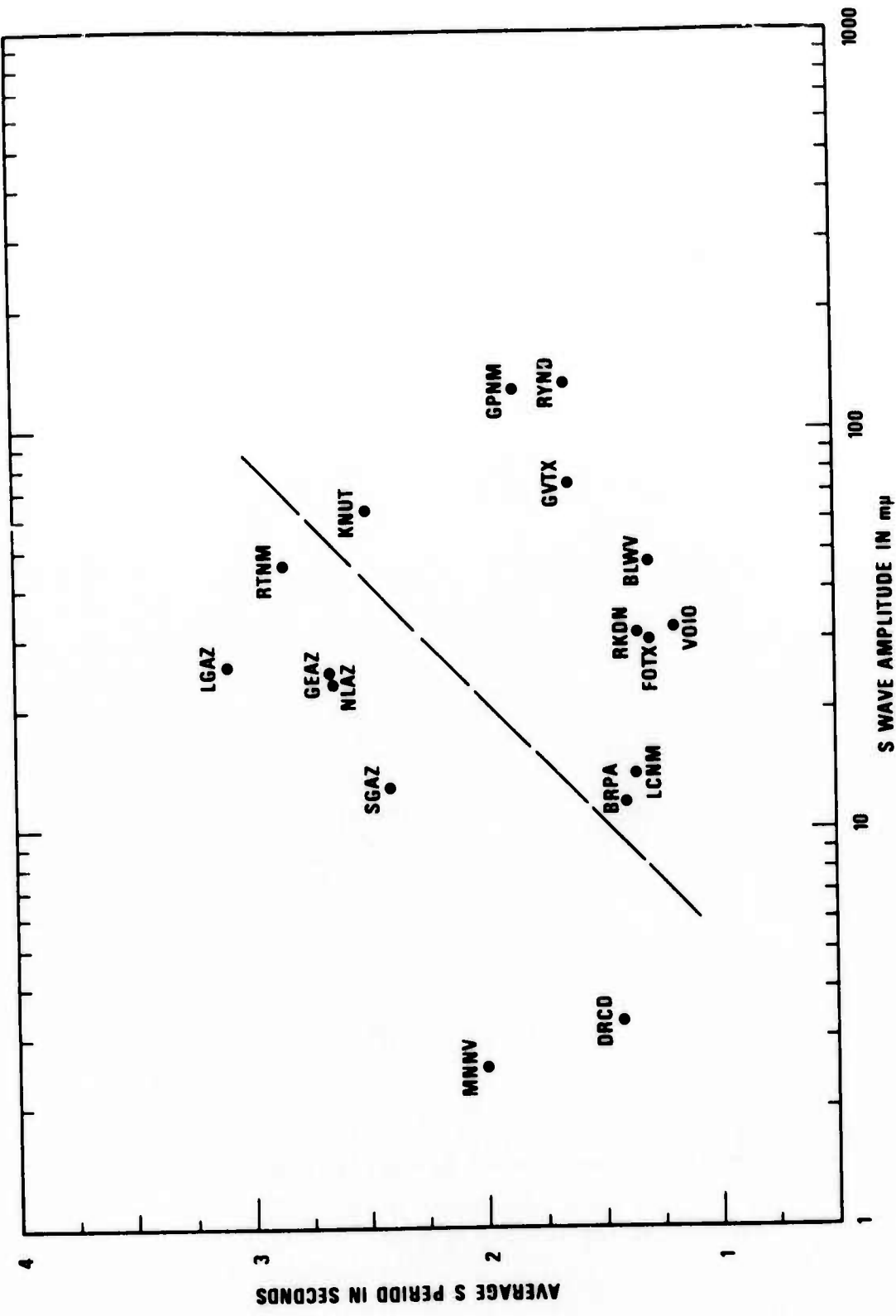


Figure 8. Dominant S wave period plotted against S wave amplitude for the Western Brazil event. Dashed line is the assumed boundary between stations with high and low attenuation.

The individual events may be considered to determine how the period measurements modify the observations based on amplitudes alone. Figure 5, which is the amplitude-period plot for the event at the Peru-Brazil border, shows that observations at stations WINV and BXUT separate from all observations at the other stations. Stations EBMT, APOK, and RYND have recorded amplitudes which are as small as those recorded at BXUT, but clearly separate on the basis of average period. Figures 6, 7 and 8 show similar results, although there is some overlap of observations such as for station LCNM in Figure 8.

P Wave Amplitudes

Inspection of Table 2 shows that, as a whole, P wave amplitudes behave in a manner similar to S waves. Evernden and Clark (1970) also found a similar pattern for P wave amplitudes. In figures 9 through 12 the logarithms of P versus S wave amplitudes are plotted for each event. This is essentially the δt_s^* plot by Solomon and Toksöz (1970). Figures 9 and 10 do not show a clear trend, but Figures 11 and 12 show a fairly clear trend indicating that P and S amplitudes are correlated for the same event. If it is assumed that the attenuation can be attributed solely to losses in shear (due to complex rigidity) and that the frequency of P is the same as that for the S waves the logarithm of amplitude values should fit a line with a slope of about .25. Remembering, however, that the average

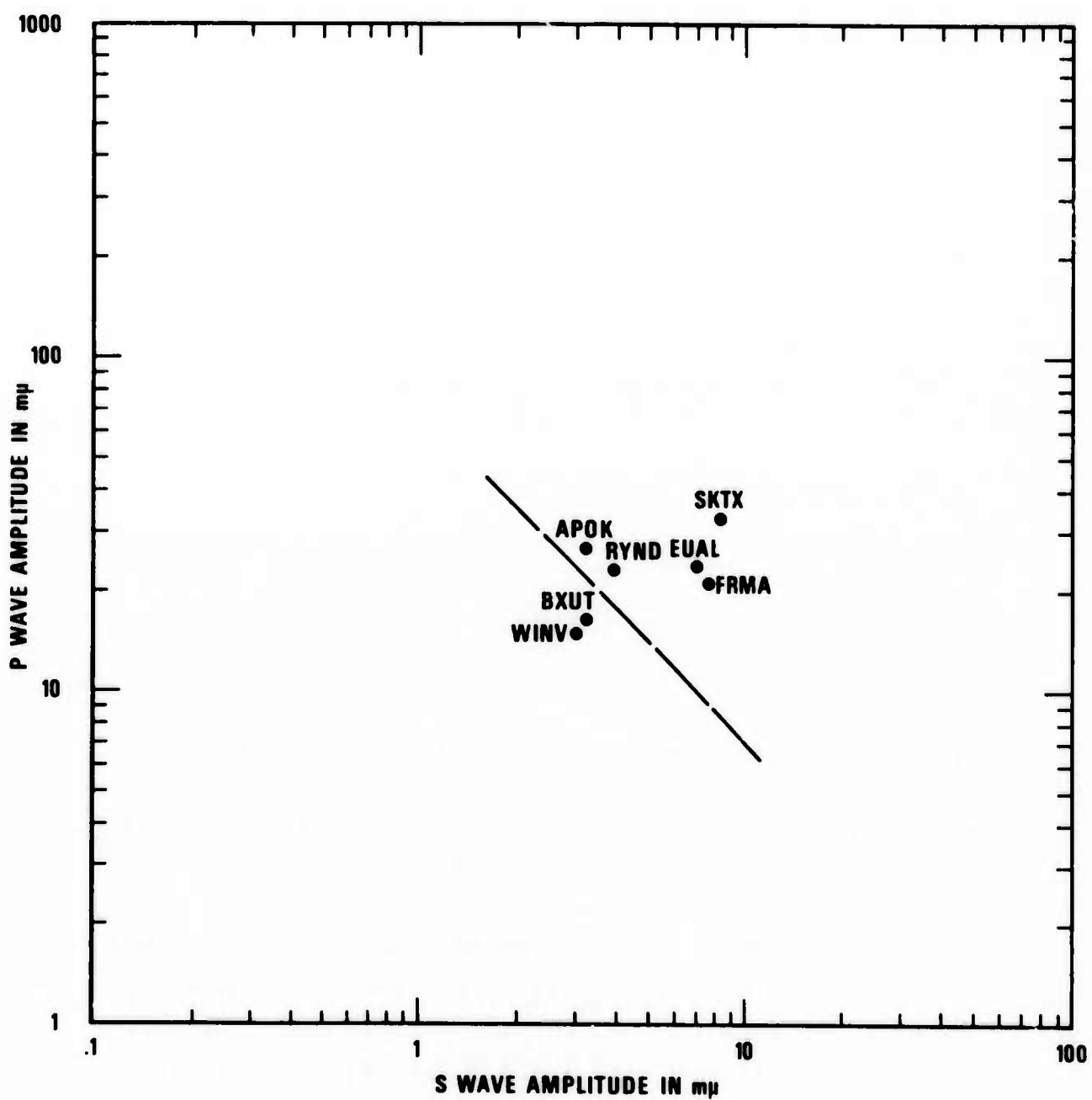


Figure 9. P amplitudes plotted against S amplitudes for the Peru-Brazil border event. Dashed line is the boundary between stations with high and low attenuation.

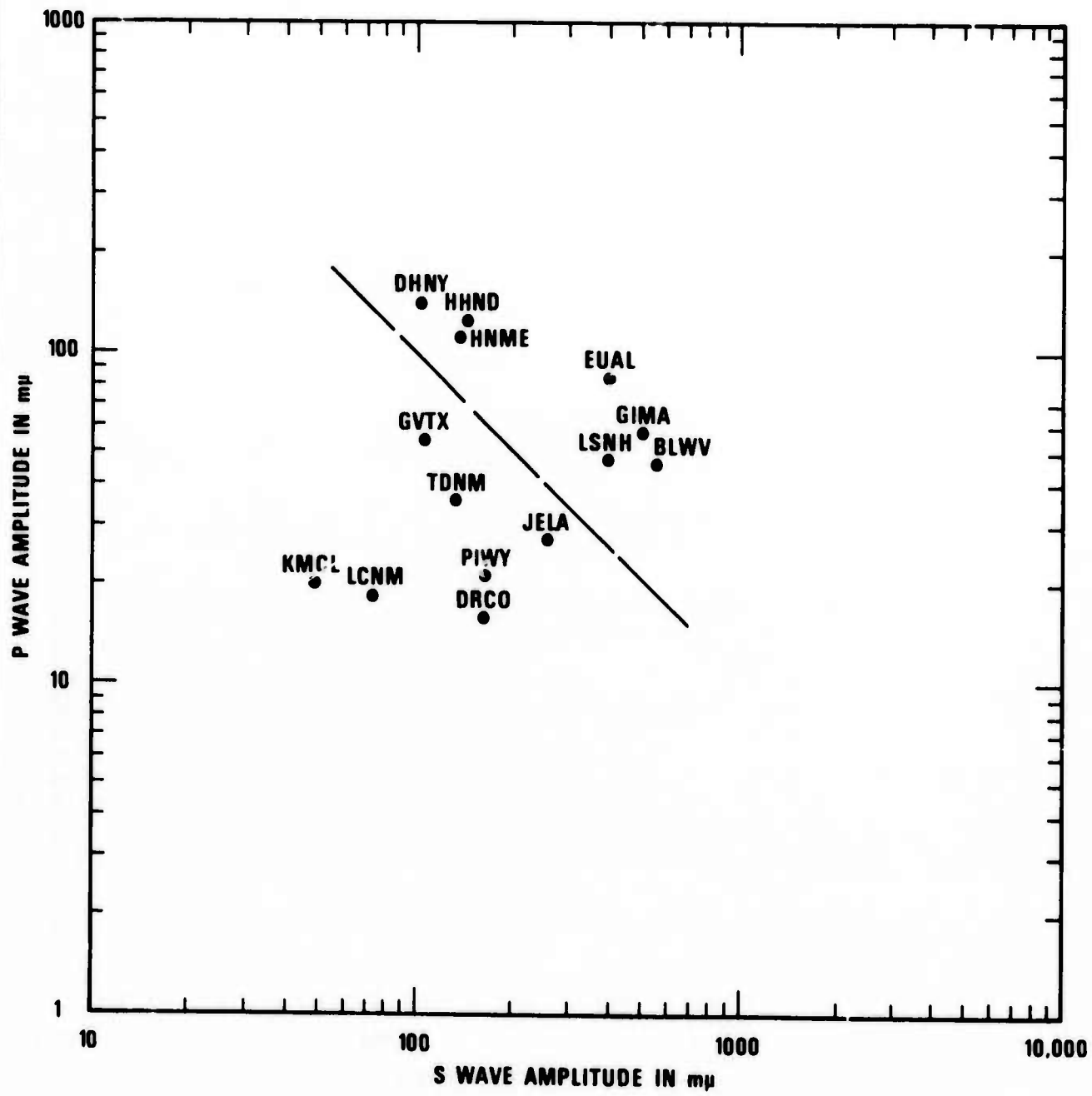


Figure 10. P amplitudes plotted against S amplitudes for the NW Kuriles event. Dashed line is the boundary between stations with high and low attenuation.

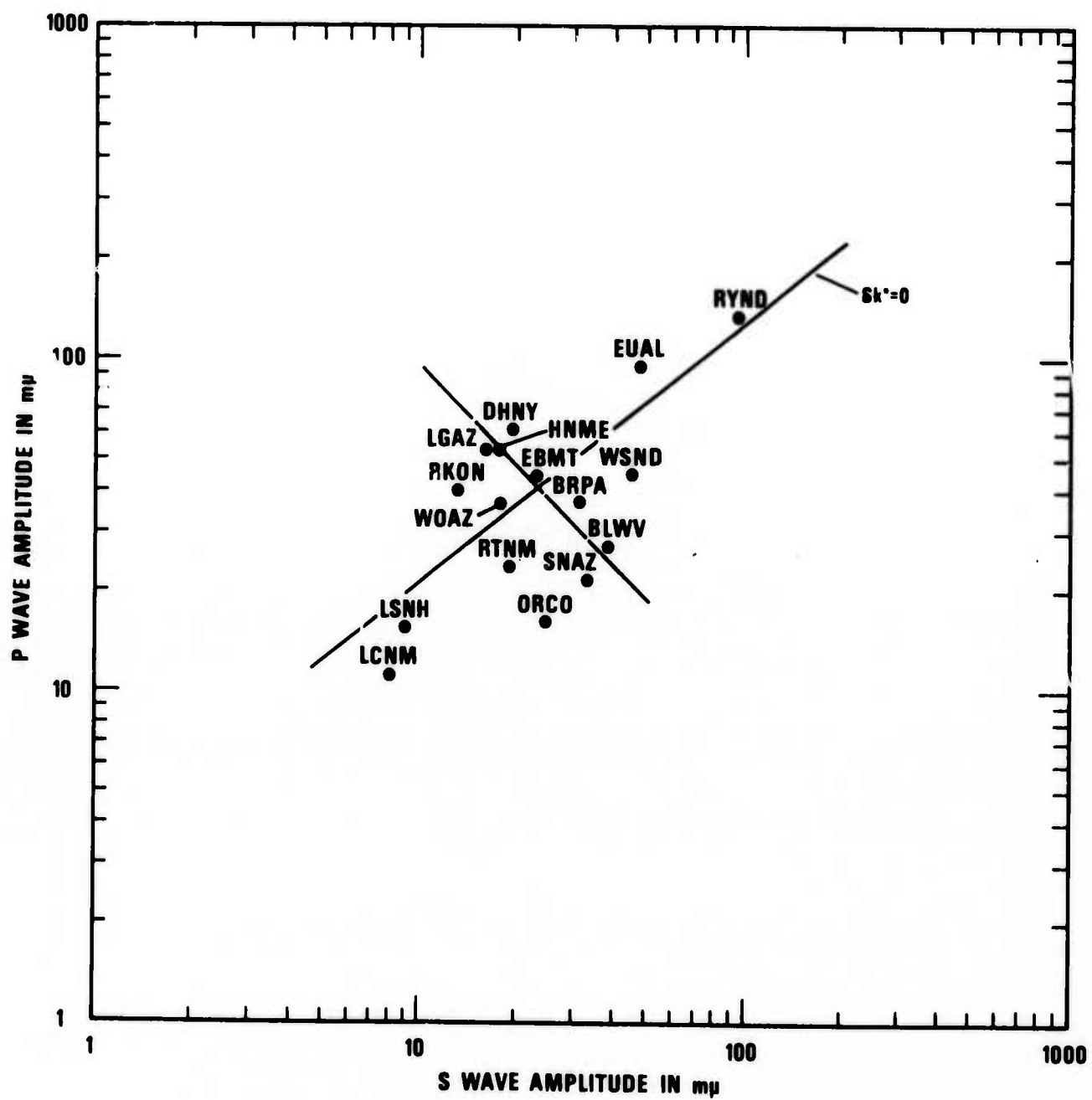


Figure 11. P amplitudes plotted against S amplitudes for the Sea of Okhotsk event. Dashed line is the boundary between stations with high and low attenuation. Solid line is the approximate relationships between P and S amplitudes assuming losses in shear only.

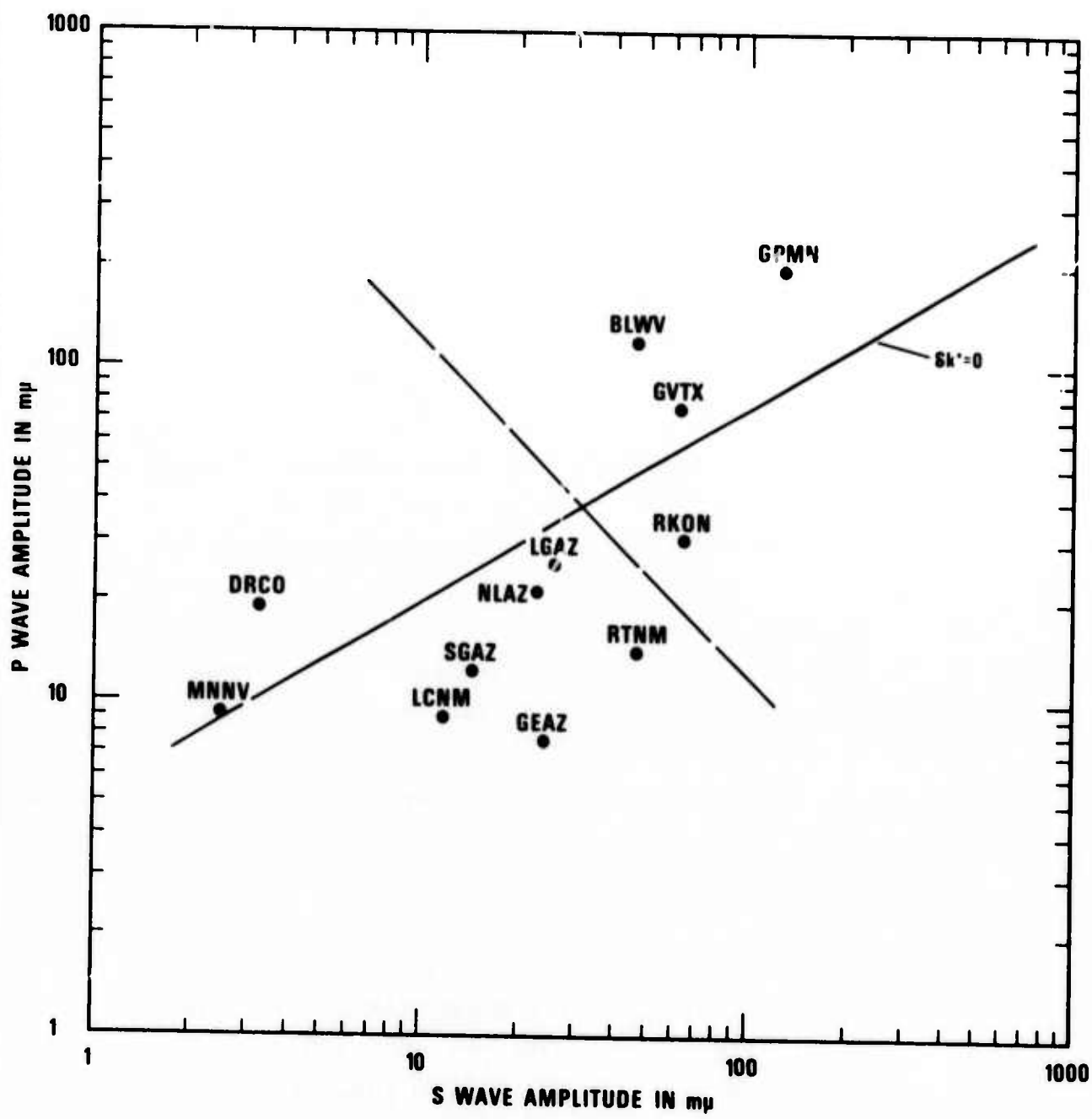


Figure 12. P amplitudes plotted against S amplitudes for the Western Brazil event. Dashed line is the boundary between stations with high and low attenuation. Solid line is the approximate relationships between P and S amplitudes assuming losses in shear only.

periods of P and S waves are different in our case, the P waves have shorter periods, and assuming a constant Q in the period range of P and S waves the slope of the line should be greater. Taking the rough average of P and S wave periods at high Q stations, these periods turn out to be about .7 and 2.1 seconds and thus the corresponding line slope about .75. For the western Brazil event the average P and S period are around .6 and 1.4 and the corresponding slope is about .6. The scatter of points in Figures 11 and 12 is such that although the fit to such lines (solid lines) is not very good it cannot be rejected with any confidence, and so it can be concluded that for the short-period waves most if not all of the energy losses are in shear and there is no need to assume that there are losses in compression. Stations in the Western United States tend to be associated with low P and S amplitudes while those in Central and Eastern United States show higher amplitudes for P and S waves.

Stations in the Northeast tend to record intermediate amplitude values.

P Wave Periods

The P wave periods (Table 2) do not behave in any consistent pattern. This can be partially attributed to the difficulty of measuring periods of high frequency P waves from film, and to the fact that P waves attenuate less and thus the dominant periods change little.

EVALUATION OF THE DATA

Although the data presented show a fairly consistent pattern, it is necessary to evaluate the average behavior of all data. Individual variables measured in this study fluctuate and none of them are sufficient to outline the attenuation pattern in detail. It can be hoped, however, that the various parameters used are not influenced in the same way by these factors. For example, S wave amplitudes and the dominant periods are influenced differently by local layering, P and S waves are influenced differently by scattering since the wave-lengths are different, and so forth. Averaging data from several events can also reduce effects due to radiation patterns.

In order to determine the average attenuation at each station, the following procedure was adopted:

- a) The scatter diagrams resulting from plotting S wave amplitudes versus periods were divided roughly halfway by a 45° upward sloping dashed line into two regions. Stations with observations close to the line were classified as intermediate (I) in attenuation, those with points in the low amplitude and long average period region as high (H) in attenuation, and those with points on the opposite side of the line as stations with low (L) attenuation; b) Plots of P amplitude versus S amplitude (Figures 9 through 12) were similarly divided by a 45° downward sloping line, and

a similar classification was used, the low P and S amplitude end of the diagram being the high attenuation side; c) In cases where one of the amplitudes could not be measured or only the noise background level was used as an upper limit, a decision was taken based on the available measurements; d) As a final step, a decision was made by taking the majority of observations to be the "true" attenuation measurement.

Table 3 shows the results of this procedure. In spite of the rather crude method used, the results are remarkably consistent. Although the decisions were based on rather arbitrarily chosen lines, it can be seen that shifting the lines and changing the slopes within reasonable limits will not change the results. The classification merely reflects the relative positions of the station points. Only in one case did we feel that it was justified to shift the dividing line to one side of the majority of points (Figure 9) since only two station readings were available from the high attenuation population.

TABLE 3
Classification of LRSMS Sites With Respect to Attenuation Characteristics

Station	Peru Brazil Border			NW Kuriles			Sea of Okhotsk			Western Brazil			Average
	A_s-T_s	A_s-A_p	Other	A_s-T_s	A_s-A_p	Other	A_s-T_s	A_s-A_p	Other	A_s-T_s	A_s-A_p	Other	
APOK	L	L-I	-	-	-	-	-	-	-	-	-	-	L
AZTX	L	-	-	-	-	-	-	-	-	-	-	-	L
BLWV	-	-	-	I	-	-	L	I	-	L	L	-	L
BRPA	-	-	-	-	L	-	I	I	-	I	-	H*	I
RXIT	H	H-I	-	H	-	-	-	-	-	-	-	-	H
CPCL	-	-	H*	-	-	-	-	-	-	-	-	-	H*
CUNV	-	-	H ^P	-	-	-	-	-	-	-	-	-	H ^P
DHNY	-	-	-	L	I-L	-	I-H	I-L	-	-	-	-	I-L
DRCO	-	-	H*	H	H	-	H	H	-	H	H	-	H
DUOK	L	-	-	-	-	-	-	-	-	-	-	-	L
EBMT	I-L	-	-	I	-	-	L	I	-	-	-	-	I
EKNV	-	-	-	H	-	-	-	-	H*	-	-	-	H
EUAL	L	L	-	L	L	-	L	L	-	-	-	-	L
FOTX	-	-	-	-	-	-	H	-	-	L	-	-	I
FRMA	I	L	-	I	-	-	-	-	-	-	-	-	I
GEAZ	-	-	-	-	-	-	-	-	-	H	H	-	H
GIMA	-	-	-	L	L	-	-	-	H*	-	-	-	L
CPMN	-	-	-	-	-	-	-	-	-	L	L	-	L
GVTX	-	-	-	I	I	-	-	-	-	L	L	-	I-L
HETX	-	-	L ^P	-	-	-	-	-	-	-	-	-	L ^P
HDPA	-	-	-	-	-	-	-	-	-	-	-	I*	I*
HHND	-	-	-	L	L	-	-	-	I*	-	-	-	L
HLID	-	-	-	-	-	-	H	-	-	-	-	H*	H
HNME	-	-	-	I	I-L	-	H	I	-	-	-	H*	I
JLLA	-	-	-	I	I	-	-	-	-	-	-	-	I
KMCL	-	-	-	H	H	-	-	-	-	-	-	-	H
KNUT	-	-	H-I*	H	H	-	-	-	H*	I	-	-	H
LCNM	-	-	-	H	H	-	H	H	-	I	H	-	H
LGAS	-	-	-	-	-	-	H	I	-	H	H	-	H
LSNH	-	-	-	L	I-L	-	H	H	-	-	-	-	I
LVLA	-	-	-	-	-	-	-	-	-	-	-	-	-
MNNV	-	-	H*	H	-	-	-	-	H*	H	H	-	H
MVCL	-	-	H*	-	-	-	-	-	-	-	-	-	H*
NLAZ	-	-	-	-	-	-	-	-	-	H	H	-	H
PIWY	-	-	-	I	H	-	-	-	-	-	-	-	I-H
RKON	-	-	-	L	-	-	L	I-H	-	L	L	-	L
RTNM	-	-	H*	-	-	-	H	H	-	H	H	-	H
RYND	L	L-I	-	L	-	-	L	L	-	L	-	-	L
SGA2	-	-	-	-	-	-	-	-	-	H	H	-	H
SKTX	L	L	-	-	-	-	-	-	-	-	-	-	L
SNAZ	-	-	-	-	-	-	H	H-I	-	-	-	-	H
TDNM	-	-	H*	H	H	-	-	-	-	-	-	-	H
TKWA	-	-	-	H	-	-	-	-	-	-	-	-	H
VOIO	-	-	-	-	-	-	-	-	-	L	-	-	L
WINV	H	H	-	-	-	-	-	-	-	-	-	-	H
WOAZ	-	-	-	-	-	-	H	I	-	-	-	-	I-H
WSND	-	-	-	-	-	-	L	L	-	-	-	-	L

L - low attenuation
I - intermediate attenuation
H - high attenuation

A_s-T_s - based on S amplitudes and periods
 A_s-A_p - based on S and P amplitude plots
Superscripts * - based on noise background
p - based on P amplitude only

DISCUSSION

The results of the present study demonstrate that in spite of the great variability of short-period observations, short-period waves can be used to obtain a fairly coherent picture of regional variations in attenuation within the upper mantle and crust. In particular, the combination of the amplitude and period measurements provides a quite consistent indicator of regional attenuation.

Observations of short-period waves presented in this paper indicate considerable attenuation in the Western United States. The general geographical pattern of the distribution of attenuation is consistent with similar observations of long-period body waves (Solomon and Toksöz, 1970). There seems to be a difference in the short-period and long-period attenuation patterns in California, where our short-period observations indicate high attenuation, but long-period S wave observations of Solomon and Toksöz (1970) indicate low attenuation. Our data also indicate the possible existence of a second, but less pronounced, attenuating region in the Northeastern United States.

Solomon (1972) modeled the general attenuation in the United States by the superposition of two relaxation mechanisms, one prevailing at shallow depths, the other at greater depth. Although present observations do not allow the verification of this idea, this implies that attenuation of short-period and long-period waves can

vary independently resulting in different geographical patterns.

The summary of the geographical distribution pattern derived from amplitude and period observations of S waves is shown in Figure 13. The eastern boundary of the high attenuation regions is not much different from that derived by Solomon and Toksöz (1970), as indicated by the dashed line. The geographical attenuation pattern presented here also correlates well with P and S wave travel time residuals which are late throughout the Western United States including California (Cleary and Hales, 1965; Doyle and Hales, 1967; Hales et al 1968; and Hales and Roberts, 1970). P wave amplitude measurements by Evernden and Clark (1970) also show the same pattern.

In the Texas panhandle (northwest Texas) the location of stations permits the definition of the boundary between the high and low attenuating regions. This boundary lies between AZTX and RTNM and must be quite sharp as evidenced by the contrasting behavior of S waves at the two stations. The observations do not permit the exact definition of the location or nature of the boundary further north. Study of Early Rise seismic profiles by Massé (1973) indicates a sharp change in the thickness of the upper mantle low-velocity layer located beneath central Nebraska. If the change in amplitude values in the Texas panhandle are associated with a change in thickness of the low-velocity channel, then this change in thickness must also be abrupt. By using the Texas panhandle point and the point found by

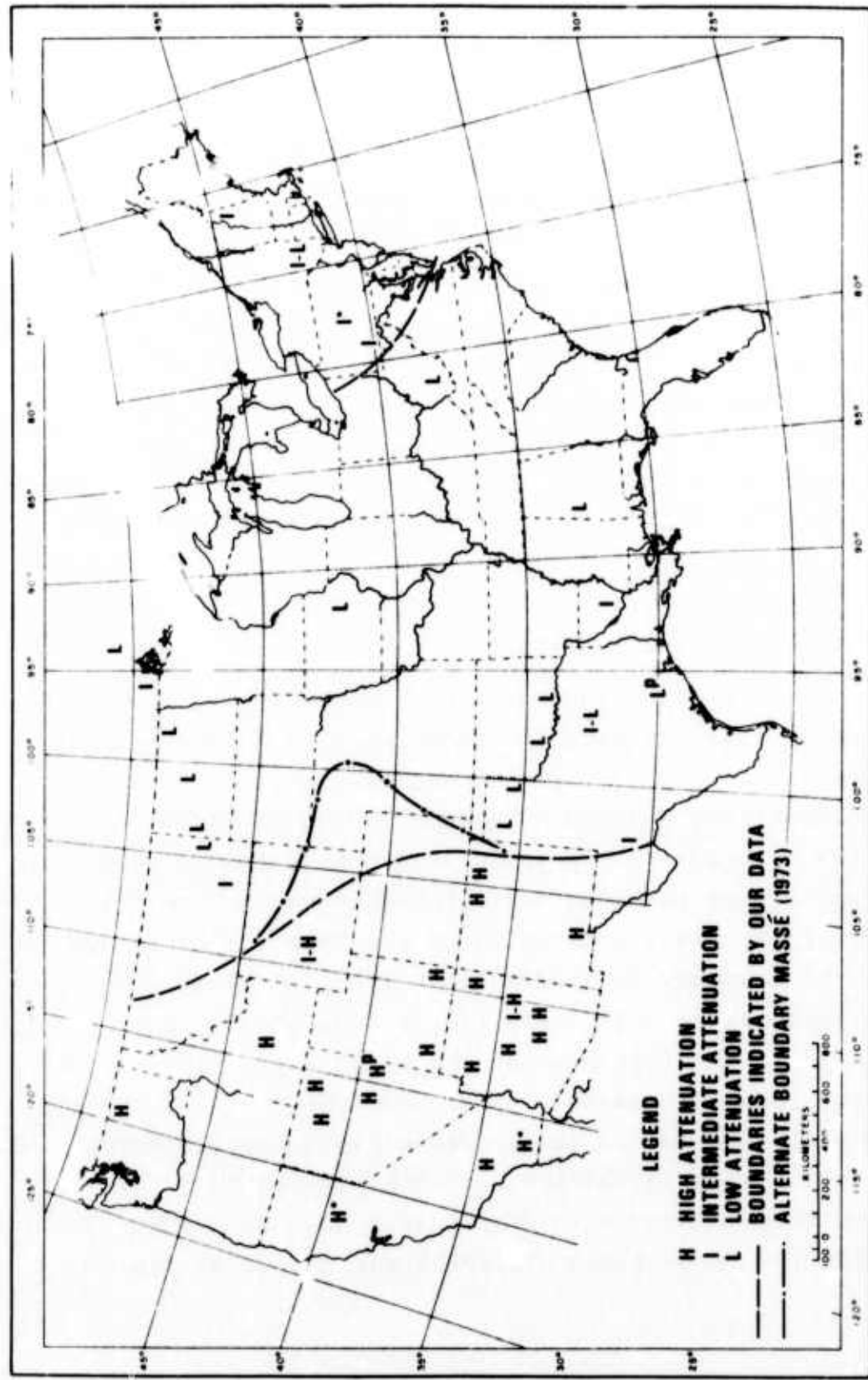


Figure 13. Distribution of attenuation under the United States based on all events.

Massé (1973) as two points which lie on the boundary between a fairly thick and a thin low-velocity channel and by correlating these points with other geophysical measurements such as heat flow (Blackwell, 1971; Combs and Simmons, 1973), a tentative boundary of the thick low-velocity layer can be drawn. This boundary line is also shown in Figure 13 (dashes and dots). This bulge in the boundary line is not required by the data presented in this paper.

Our data is also in agreement with studies of upper mantle conductivity using geomagnetic variations (Gough and Porath, 1970; Porath and Gough, 1971; Gough, 1973). The boundary line of Gough (1973) falls somewhat to the west of ours, and some regions of high attenuation, California and the Colorado plateau for example, have low conductivity. It must be remembered, however, that measurements of conductivity reflect the variations in the depth of the upper boundary of the conducting region while body waves sample the total thickness of the upper mantle, thus no complete correlation between the two types of measurements can be expected. The same general remarks apply to heat flow measurements also (Blackwell, 1969, 1971). The results of Archambeau, Flinn and Lambert (1969) also indicate a variation in the depth of low velocity material in the mantle of the Western United States.

The region of higher attenuation in the northeast is less pronounced than that for long-period and its

boundaries are not well defined. On the period-amplitude plots the stations in this region occupy intermediate values between those of low and high attenuation regions.

The relative attenuation of short-period P and S waves is consistent with losses which are only in shear with no loss in compression. Differences in the attenuation patterns of short-period waves relative to long-period waves indicate that the average attenuation mechanism changes as a function of geographical position, although it can not be ascertained whether the attenuation of short and long-period waves occurs at different depths. Mapping relative attenuation as a function of period and geographical position can be an important tool in exploring the upper mantle. Variation of attenuation also influences the detectability and character of various phases and thus have a direct bearing on studies dealing with source spectra and discrimination of earthquakes and explosions.

Attenuation of the direct arrival of short period seismic waves through low Q regions as demonstrated in this paper coupled by nonminimum time arrivals through the high Q lithosphere can account for the changes in the complexity of signals as proposed by Douglas et al (1973). The complexity of signals was not investigated in this paper, but it seems to be a worthwhile research topic for the future.

ACKNOWLEDGEMENTS

We wish to thank Drs. R. R. Blandford and E. A. Flinn for reviewing the paper and offering valuable suggestions.

REFERENCES

Anderson, D. L. and Archambeau, C. B., 1964. The anelasticity of the earth: *J. Geophys. Res.*, v. 69, p. 2071-2084.

Anderson, D. L., Ben-Menahem, A. and Archambeau, C. B., 1965. Attenuation of seismic energy in the upper mantle: *J. Geophys. Res.*, v. 70, p. 1441-1448.

Archambeau, C. B., Flinn, E. A. and Lambert, D. H., 1969. Fine structure of the upper mantle: *J. Geophys. Res.*, v. 74, p. 5825-5865.

Blackwell, D. D., 1969. Heat flow determinations of the northwestern United States: *J. Geophys. Res.*, v. 74, p. 992-1007.

Blackwell, D. D., 1971. Heat flow: *Trans. Am. Geophys. Un.*, v. 52, IUGG 135-IUGG 139.

Cleary, J. and Hales, A. L., 1966. An analysis of the travel times of P waves to North American stations, in the distance range 32° to 100° , *Bull. seism. Soc. Am.*, v. 56, p. 467-489.

Combs, T. and Simmons, G., 1973. Terrestrial heat flow determinations in the north central United States: *J. Geophys. Res.*, v. 78, p. 441-461.

Douglas, A., Marshall, P. D., Gibbs, P. G., Young, I. B. and Blamey, C., 1973. P signal complexity re-examined: *Geophys. J. R. astr. Soc.*, v. 33, p; 195-222.

REFERENCES (Continued)

Doyle, H. A. and Hales, A. L., 1967. An analysis of the travel times of S waves to North American stations in the distance range 28° to 82° : Bull. Seism. Soc. Am., v. 57, p. 761-771.

Evernden, J. F. and Clark, E. M., 1970. Study of teleseismic P II amplitude data: Phys. Earth. Planet. Interiors, v. 4, p. 24-31.

Gough, D. I. and Porath, H., 1970. Evidence for a long-lived thermal structure under the southern Rocky Mountains: Nature, v. 226, p. 837-839.

Gough, D. I., 1973. The geophysical significant of geomagnetic variation anomalies: Phys. Earth. Planet. Int., v. 7, p. 379-388.

Hales, A. L. and Doyle, H. A., 1967. P and S travel time anomalies and their interpretation: Geophys. J. R. astr. Soc., v. 13, p. 403-415.

Hales, A. L., Clery, J. R., Doyle, H. A., Green, R., and Roberts, J., 1968. P wave station anomalies and the structure of the Upper Mantle, J. Geophys. Res., v. 73, p. 3885-3896.

Hales, A. L. and Roberts, J., 1970. The travel times of S and SKS: Bull. Seism. Soc. Am., v. 60, p. 461-489.

Jackson, D. D., 1969. Elastic relaxation model for seismic wave attenuation in the earth: Phys. Earth. Planet. Int., v. 2, p. 30-34.

Masse, R. P., 1973. Compressional velocity distribution beneath central and eastern North America: Bull. Seism. Soc. Am., v. 63, p. 911-935.

REFERENCES (Continued)

Molnar, P. and Oliver, J., 1969. Lateral variations of attenuation in the upper mantle and discontinuities in the lithosphere: *J. Geophys. Res.*, v. 74, p. 2648-2682.

Oliver, J. and Isacks, B., 1967. Deep earthquake zones, anomalies structures in the upper mantle and the lithosphere: *J. Geophys. Res.*, v. 72, p. 4259-4275.

Porath, H. and Gough, D. I., 1971. Mantle conductive structures in the Western United States from magnetometer array studies: *Geophys. J. R. astr. Soc.*, v. 22, p. 261-275.

Solomon, S. C. and Toksöz, M. N., 1970. Lateral variation of attenuation of P and S waves beneath the United States: *Bull. Seism. Soc. Am.*, v. 60, p. 819-838.

Solomon, S. C., Ward, R. W. and Toksöz, M. N., 1970. Earthquake and explosion magnitudes, the effect of lateral variation of seismic attenuation, Wood's Hole Conference on Seismic Discrimination, Working Paper.

Solomon, S. C., 1972. Seismic-wave attenuation and partial melting in the upper mantle of North America: *J. Geophys. Res.*, v. 77, p. 1483-1502.

Sato, R. and Espinosa, A. F., 1967. Dissipation in the Earth's mantle and rigidity and viscosity in the

REFERENCES (Continued)

Earth's core determined from waves multiply reflected from the mantle-core boundary: Bull. Seism. Soc. Am., v. 57, p. 829-856.

Sutton, G. H., Mitronovas, W. and Pomeroy, P. W., 1967. Short period seismic energy radiation patterns from underground nuclear explosions and small magnitude earthquakes: Bull. Seism. Soc. Am., v. 57, p. 249-267.

Walsh, J. B., 1968. Attenuation in partially melted material: J. Geophys. Res., v. 73, p. 2209-2216.